DOI 10.1007/s10812-018-0603-y
Journal of Applied Spectroscopy, Vol. 85, No. 1, March, 2018 (Russian Original Vol. 85, No. 1, January–February, 2018)

INFLUENCE OF INTERMOLECULAR INTERACTIONS AND AXIAL LIGANDS ON THE ABSORPTION SPECTRA OF METALLOPHTHALOCYANINES IN SOLID-STATE MATRICES

T. A. Pavich,[a] S. M. Arabei,[b*] and K. N. Solovyov[a]

UDC 535.37;535.34

The influences of the structure of the anionic axial ligands in Group-IIIA and -IVA metal–phthalocyanine complexes and intermolecular interactions on the absorption spectra of the macroheterocycles in solutions, an organic polymer, and nanoporous silicate gel matrices were studied. It was shown that anionic Cl^- ligands of the central metal ion were effectively substituted for hydroxyls (OH^-) during the synthesis and purification of the metallophthalocyanines. Studies of solid-state nanoporous samples obtained by the sol-gel method showed that activator hydroxoaluminum-phthalocyanine molecules were incorporated as monomers into the organo-inorganic silicate material. The optically homogeneous luminescent xerogel could be used in optical devices for the wavelength range adjacent to the near-IR region.

Keywords: *metallophthalocyanines, sol-gel synthesis, nanoporous silicate matrices, electronic absorption spectrum, IR spectrum, ligand exchange, monomeric and aggregated forms.*

Introduction. Phthalocyanines, which are also called tetrabenzoporphyrazines (porphyrazine is the same as tetraazaporphine), possess an extensive conjugated π-electron system and have high chemical resistance and thermal stability. Previously, phthalocyanines and their metal complexes (further MPc, without isolating the free base phthalocyanine H_2Pc) were investigated in detail mainly as light-resistant dyes and pigments. Recently, these compounds and the related naphthalocyanines have attracted attention as materials with nontraditional physical properties for many applications, e.g., liquid crystals [1], nonlinear optical materials [2–4], gas sensors [5], catalysts [6], electrochromic devices [7], etc. MPc are also used as photosensitizers in photodynamic therapy and diagnostic fluorescence to treat oncological diseases [8, 9].

Utilization of the structural and physicochemical properties of the monomers of these compounds provides a basis for discovering and developing practically useful systems based on MPc. The monomers give narrow absorption and fluorescence bands in the wavelength range adjacent to the near-IR region and can have high fluorescence quantum yields. Conversely, aggregation of MPc causes strong fluorescence quenching and washout of the absorption spectrum, preventing their practical application. This circumstance stimulated a search for MPc capable of existing as the monomeric species in various solvents, which entailed a study of the structure and properties of the macroheterocycle–environment system. The problem of introducing monomeric MPc activators into media that should be solids for practical purposes is closely related to the solubilities and intermolecular interactions of the macroheterocycles. Inorganic matrices, primarily silicate glasses, have advantages over organic polymers with respect to mechanical strength, light resistance, and service life. Silicate matrices and films can be activated in two ways, i.e., soaking the finished nanoporous structure and direct sol-gel synthesis from a solution containing the activator. Our group has over several years used spectroscopy to investigate tetrapyrroles in silicate gel-marices and gel-films [10].

The present work studied the possibility of incorporating MPc monomers into silicate gel-matrices using Group-IIIA and -IVA metal phthalocyanine complexes considering the shielding effect of the axial ligands.

Experimental. Silicon dichloride phthalocyanine ($SiCl_2Pc$) was prepared from 1,3-diiminoisoindoline and $SiCl_4$ in quinoline using a slightly modified method [11–13]. Other MPc were prepared using 1,2-phthalonitrile as the starting precursor. Germanium dichloride phthalocyanine ($GeCl_2Pc$) was prepared by the published method [13, 14].

*To whom correspondence should be addressed.

[a]B. I. Stepanov Institute of Physics of the National Academy of Sciences of Belarus, Minsk; [b]Belarusian State Agrarian and Technical University, 99 Nezavisimost′ Ave., Minsk, 220023, Belarus; email: arabei.chemistry@bsatu.by.
Translated from Zhurnal Prikladnoi Spektroskopii, Vol. 85, No. 1, pp. 5–13, January–February, 2018. Original article submitted April 28, 2017.

Aluminum chloride phthalocyanine (AlClPc) was synthesized as before for AlCl-tetra(2,3-anthra)-porphyrazine [15]. The gallium complex of phthalocyanine (GaClPc) was synthesized by an analogous method, i.e., using 1,2-phthalonitrile and $GaCl_3$. The synthesized metal complexes were purified by heating the MPc powders in a vacuum sublimator at 400–420°C for 2 h at reduced pressure (10^{-3} Torr), i.e., vacuum sublimation, although they partly decomposed in the process.

Electronic absorption spectra (EAS) were measured on a Cary-500 Scan spectrophotometer (Varian, USA). All EAS except for that of the Al phthalocyanine complex in EtOH were taken without a reference channel. IR spectra of KBr pellets were measured on a Nexus FTIR spectrometer (Thermo Nicolet, USA) with resolution ~4 cm^{-1} by averaging 128 scans followed by baseline linearization.

Polyvinylbutyral (PVB), a synthetic polymer supplied by industry as a white powder, was chosen as the organic polymer and solid-state matrix for incorporation of MPc. PVB samples were prepared as thin optically transparent films with the colors of the synthesized MPc by pouring an EtOH solution of the chosen film-forming polymer onto a horizontal glass substrate. This provided films with even thicknesses although the films were unavoidably thicker along the substrate edges. Film formation was finalized by drying. The film thickness was adjusted by the number of repeated pourings, which depended on the viscosity of the EtOH solution of the polymer. The obtained polymer films were formed by 3–4 pourings. The final thicknesses of the dried colored PVB films were 100–500 μm.

Silicate glass has attracted attention as an inorganic nonmetallic material because of its thermal longevity and chemical inertness. The glass is produced at temperatures >700°C. However, many modern electronic or optical devices require silicate glasses doped with organic dyes, which cannot be processed at high temperatures. This problem was solved by using sol-gel processes at room temperature to form the materials from solutions. This new technology was developed for solid-state silicate materials.

Sol-gel processes are chemical reactions that start with the hydrolysis of monomeric tetrafunctional alkoxides of the corresponding chemical elements by adding H_2O in the presence of an inorganic acid or base as a catalyst. The alkoxides used most often for Si are tetramethoxysilane $Si(OMe)_4$ (TMOS) and tetraethoxysilane $Si(OEt)_4$ (TEOS). The alkoxide groups (–OR) of the starting Si alkoxides with Si–OR groups are replaced by hydroxyls (–OH) in the first reaction step:

$$Si(OR)_n + H_2O \leftrightarrows (RO)_{n-1}Si(OH) + ROH\ .$$

Polycondensation begins in most instances before the hydrolysis is complete and results eventually in the formation of a 3D polymer network. The polycondensation can occur either at silanols (Si–OH), which react with each other to form siloxane bonds (≡Si–O–Si≡) and release H_2O (transformation of two hydroxyls into an oxygen bridge):

$$(RO)_{n-1}Si(OH) + (HO)Si(OR)_{n-1} \rightarrow (RO)_{n-1}Si{-}O{-}Si(OR)_{n-1} + H_2O$$

or at a silanol and alkoxide, which also form siloxane bonds (≡Si–O–Si≡) but release alcohol (alkoxylation):

$$(RO)_{n-1}Si(OH) + (RO)Si(OR)_{n-1} \rightarrow (RO)_{n-1}Si{-}O{-}Si(OR)_{n-1} + ROH\ .$$

Thus, low-temperature hydrolysis and condensation even in the early stages form a 3D polymer framework where the inner Si atoms are connected through Si–O–Si bonds although the outer Si atoms have at least one Si–OH bond.

Silicates prepared using the sol-gel process have porous structures because the finished material is a gel. Its pores contain solvents, H_2O, and alcohol, formed from the starting Si alkoxide. A solid forms after gelation and drying and has a multitude of OH groups on nanopore surfaces. Residual alkoxide OR groups can also be present in the material. These groups react with each other during curing of the matrix to form additional amounts of H_2O and alcohol. Ultimately, a material with a 3D nanoporous structure is synthesized. Based on this, sol-gel materials are classified as nanomaterials.

Modifications of the materials that are impossible for classical high-temperature silicate synthesis can occur under the mild conditions of the sol-gel process. For example, organic molecules or biological components can be incorporated by adding the corresponding solutions to the sol-gel reaction mixture because of the low temperature and the presence of solvents in the material. Furthermore, hybrid organo-inorganic materials produced by combined hydrolysis and polycondensation of chemically different starting Si alkoxides containing organic functional groups [e.g., vinyltriethoxysilane (VTEOS)] that are not hydrolyzed and end up bound to the inorganic lattice on the surface of matrix nanopores can be synthesized using the sol-gel process.

The present work reports the sol-gel synthesis of 3D inorganic (based on TEOS) and organo-inorganic (based on a mixture of TEOS and VTEOS) gel matrices activated by MPc. Commercial TEOS and VTEOS (Sigma-Aldrich) were used without further purification.

TEOS gel matrices were prepared via hydrolysis and condensation of TEOS in aqueous alcohol with a molar ratio TEOS:EtOH:H_2O:formamide = 1:5:5:5. The reaction mixture was treated with HCl (~0.1 mol) to accelerate the hydrolysis and stirred for 4 h until a homogeneous solution formed (start of hydrolysis stage). Organo-inorganic xerogels were prepared from a mixture of TEOS and VTEOS in a 70:30% mole ratio. The molar ratio of components was (TEOS + VTEOS):H_2O:EtOH:formamide = (0.7 + 0.3):5:5:5. Several drops of HCl were added after stirring for 30 min. Then, the resulting mixture was stirred for an additional ~5 h.

The reaction mixtures were stored at room temperature for 1 day so that the hydrolysis could proceed. Then, the reaction mixtures with an initial acidic pH (~4) were stirred vigorously and treated dropwise with NH_3 in EtOH at pH 8 to adjust the reaction mixture to pH ~7. The pH had to be shifted toward neutral to accelerate the polycondensation and prevent partial decomposition of MPc in the acidic solution. The prepared reaction mixtures were poured into plastic cuvettes, treated with saturated solutions of MPc in DMF, sealed tightly with film, and left at room temperature in the dark. Solid xerogel formed over the course of several weeks (polycondensation stage) and had a silicate framework with pores incorporating dopant MPc molecules. The plastic cuvettes were opened to remove volatile components (H_2O, EtOH, DMF) from the synthesized gels. The synthesized colored TEOS and TEOS + VTEOS gel matrices were stored for a long time (60 d) at room temperature at atmospheric pressure. Drying caused noticeable shrinkage (up to 50–70% of the initial volume) of the synthesized silicate gel matrices.

Results and Discussion. *EAS of MPc in solvents.* A general comment needs to be made before the obtained EAS results are discussed. An important methodical result was obtained during studies on SiPc oligomers [13]. The EAS of $SiCl_2Pc$ with the *Q*(0–0)-band maximum at 699 nm in anhydrous Py converted into the spectrum of $Si(OH)_2Pc$ with a maximum at 671 nm upon exposure to atmospheric moisture for 24 h. In other words, the complex was readily hydrolyzed in solution if special drying measures were not taken. This explained discrepancies in results of various researchers. The same could occur for MPc of other Group-IIIA and -IVA metals. A review already in 1975 of metalloporphyrins confirmed that hydroxo complexes could be most easily isolated for M = Al(III) in addition to Ga(III), Cr(III), Si(IV), Ge(IV), and Sn(IV) [16].

Table 1 presents the EAS in order to compare them with the literature. The extremely low solubility of many MPc limits the volume of information on the solvent effect on the EAS. Table 1 includes wavelengths for *Q*(0–0)-bands λ_{cln} in chloronaphthalene; λ_{Py} in Py, and λ_{DMF} in DMF. The volume of corresponding information could be increased by using data for λ^{tb} of tetra(*tert*-butyl)-substituted MPc^{tb} analogs. Experiments showed that λ^{tb} was greater than λ by 5–6 nm for complexes of the same metal. Therefore, Table 1 contains λ and λ', where $\lambda' = (\lambda^{tb} - 6)$ nm. The usefulness of this approach is clear from the data for H_2Pc and CuPc. Furthermore, data for solvents with influences on the EAS similar to those of the three aforementioned solvents were taken from a catalog [17] (without citation) and a review [18].

The situation with the Si complexes given in Table 1 is clear based on the aforementioned data. Few data exist for the Ge complexes although a bathochromic shift was confirmed on going from $Ge(OH)_2Pc$ to $GeCl_2Pc$. The quantity λ'_{bz} for $GeCl_2Pc^{tb}$ in benzene should be close to λ_{Py} for $GeCl_2Pc$. The shift was 16 nm whereas it was greater (28 nm) for the Si complexes in Py. The situation with complexes of Group IIIA metals, especially Ga, was even worse. Apparently, several researchers working with commercial companies did not consider the possibility of ligand exchange. A bathochromic shift of ~13 nm occurred for AlOHPc (λ_{Py} = 677 nm) and $AlClPc^{tb}$ (λ'_{tol} = 690 nm). However, λ_{cln} = 691 nm for AlClPc was 5 nm less than λ'_{cln} for $AlClPc^{tb}$ (an atypical difference, the shift could be less). Careful predictions based on the data in Table 1 give λ_{DMF} of 683–685 nm for AlClPc and not 677 nm as before [21]. Data for the Ga complexes are contradictory. The λ_{cln} value was indicative of a large bathochromic shift for GaClPc; the λ_{Py} and λ_{DMF} values, of hydroxylation. However, the literature gives λ_{DMF} = 684 nm for GaOHPc, i.e., greater than for GaClPc. It was important for our experiments that drying measures were not taken. The sol-gel synthesis occurred in an aqueous phase, i.e., mainly hydroxyl complexes were involved.

Figure 1 shows EAS of MPc solutions at room temperature. The spectra consisted of a strong absorption band in the visible region at ~670 nm that is usually called the *Q*(0–0)-band and a band in the near-UV region at ~350 nm that is called the Soret band or a *B*-band by analogy with metalloporphyrins. It was shown that the central metal with anionic axial ligands and solvents had different influences on the absorption-band positions, especially the *Q*(0–0)-band.

The experimental and literature data agreed according to a comparison of Fig. 1 and Table 1. Thus, the EAS of the Si complex in Py (Fig. 1a, curve 2) agreed well with the literature data [13] for $Si(OH)_2Pc$. The weak band at 699 nm could indicate the presence of $SiCl_2Pc$ in solution, as reported before [13]. The EAS of $Si(OH)_2Pc$ in DMSO (curve 3) also agreed with the literature [20] (Table 1).

TABLE 1. Influence of Solvent on Absorption of the $Q(0–0)$-band of MPc (λ, nm) and MPc^{tb} ($\lambda' = \lambda^{tb} - 6$ nm) from the Literature [17, 18] and the Newest Data

MPc	Chloronaphthalene (λ_{cln}, λ'_{cln})	Py (λ_{Py}, λ'_{Py})	DMF (λ_{DMF}, λ'_{DMF})
H_2Pc	698	694	–
H_2Pc^{tb}	697′	694′	$691'_{mma}$
CuPc	678	–	–
$CuPc^{tb}$	678′	$671'_{tol}$, $669'_{DMSO}$	$667'_{mma}$
$SiCl_2Pc$	682	699	–
$Si(OH)_2Pc$	–	671 [13], 672_{bz} [19], 672_{DMSO} [20]	667_{thf} [19]
$GeCl_2Pc$	696	–	–
$GeCl_2Pc^{tb}$	–	$692'_{bz}$	–
$Ge(OH)_2Pc$	–	676 [13], 676_{DMSO} [20]	–
AlClPc	691	681_{DMSO} [21]	677 [21], 675_{thf} [21]
$AlClPc^{tb}$	696′	$690'_{tol}$, $667'_{DMSO}$	–
AlOHPc	–	677 [22]	672 [23], 677_{thf} [21]
GaClPc	700, 702_{nb}	680_{DMSO} [24, 25]	678 [24], 677_{thf} [24]
$GaClPc^{tb}$	–	687′ [26]	$683'_{mma}$
GaOHPc	–	–	684 [23]

Note. nb is nitrobenzene; bz, benzene; tol, toluene; DMSO, dimethylsulfoxide; thf, tetrahydrofuran; and mma, methyl methacrylate.

The position of the $Q(0–0)$-band of $Ge(OH)_2Pc$ in Py (Fig. 1b, curve 2) agreed with the literature [13]. However, the EAS was complicated by the appearance of additional absorption bands that were attributed to the presence of aggregates. The low solubilities of MPc are known to be responsible for the strong tendency of their molecules to aggregate [27] (see below). The contribution of short-wavelength aggregates was greater in DMF. The bathochromic shift of 7 nm on going from DMF to Py was slightly greater than usual.

The EAS of AlOHPc in DMF [$Q(0–0)$-band at 674 nm] agreed with the data in Table 1. The EAS lacked signatures of aggregation. The position of the $Q(0–0)$-band (676 nm) for the Ga complex in DMF agreed with the value of 678 nm for GaClPc [24] whereas the corresponding value was 684 nm for GaOHPc. The issue required further study.

IR spectra of MPc with Si and Ge were recorded to confirm that ligand exchange occurred (Fig. 2). According to the literature [13, 19, 28, 29], the IR spectrum of $SiCl_2Pc$ has a very strong band at 468 cm^{-1} and a medium band at 692 cm^{-1} that are missing in the IR spectrum of $Si(OH)_2Pc$ in Fig. 2. Also, the IR spectrum of $Si(OH)_2Pc$ has a weak band at 451 cm^{-1} (curve 1) that is consistent with replacement of anionic Cl^- ligands by hydroxo groups, i.e., $Si(OH)_2Pc$, according to the literature [13, 19, 28, 29]. A very strong band at 830 cm^{-1} (curve 1) was missing in spectra of $SiCl_2Pc$ [13, 19, 28, 29] and belonged to Si–OH antisymmetric stretching vibrations in $Si(OH)_2Pc$. These data led to the conclusion that the IR spectra shown in Fig. 2 corresponded in fact to IR spectra of $Si(OH)_2Pc$ and $Ge(OH)_2Pc$.

EAS of MPc in solid-state matrices. As noted above, luminescent materials for the visible and near-IR regions that were developed from the MPc used in the work had practical value if the MPc could remain as monomers in various solid-state matrices, i.e., when practically useful systems utilized the structural, spectral, and physicochemical properties of the monomeric forms of these compounds. Next, spectra data (EAS) obtained for solid-state materials based on thin organic polymer PVB-films, inorganic TEOS, and hybrid TEOS + VTEOS silicate gel matrices colored by Group-IIIA and -IVA metal phthalocyanine complexes were analyzed. The EAS could be used to draw conclusions about MPc aggregation because spectra of monomeric, dimeric, and polymeric aggregated MPc are known to differ considerably [27]. This approach provided a basis for interpreting the EAS of the colored materials shown in Fig. 3.

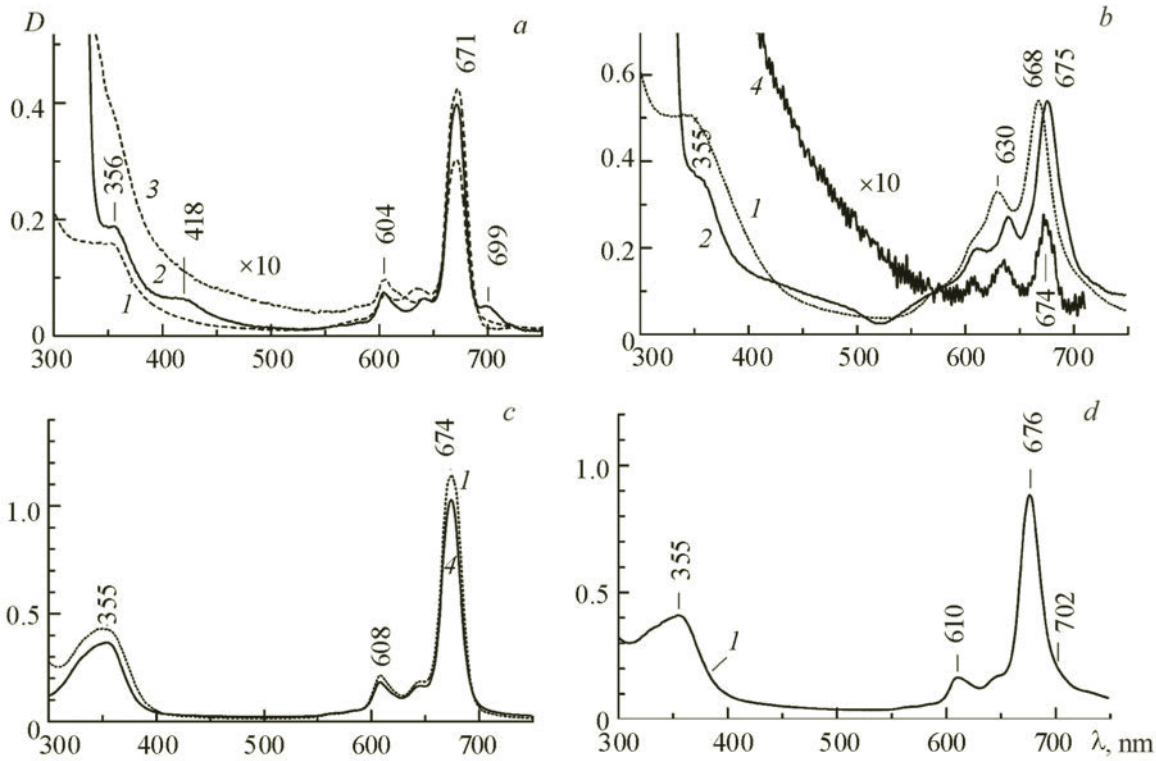

Fig. 1. Electronic absorption spectra of $Si(OH)_2Pc$ (a), $Ge(OH)_2Pc$ (b), AlOHPc (c), and GaOHPc (d) in DMF (1), Py (2), DMSO (3), and EtOH (4) at 300 K.

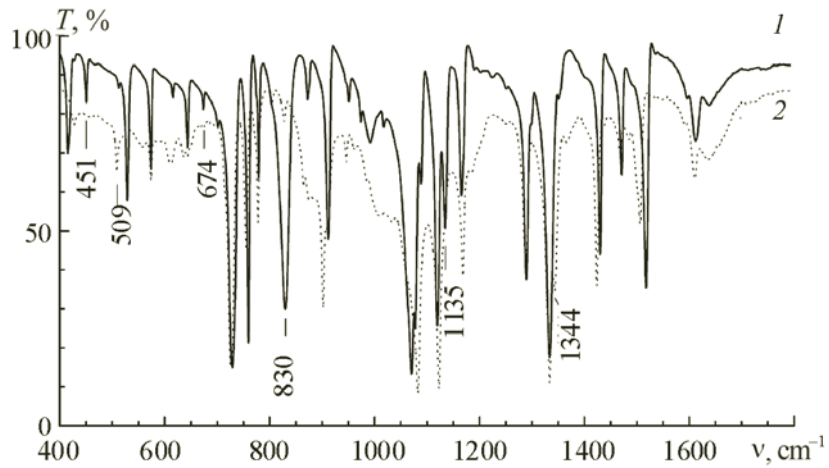

Fig. 2. IR spectra of $Si(OH)_2Pc$ (1) and $Ge(OH)_2Pc$ (2) in KBr.

Therefore, $SiCl_2Pc$ was hydrolyzed by H_2O during its synthesis and purification in undried solvents to give $Si(OH)_2Pc$ according to the reaction:

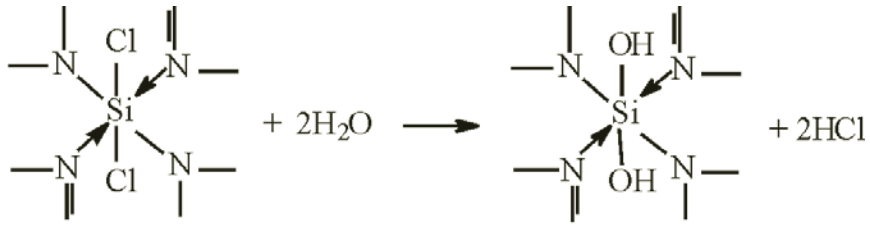

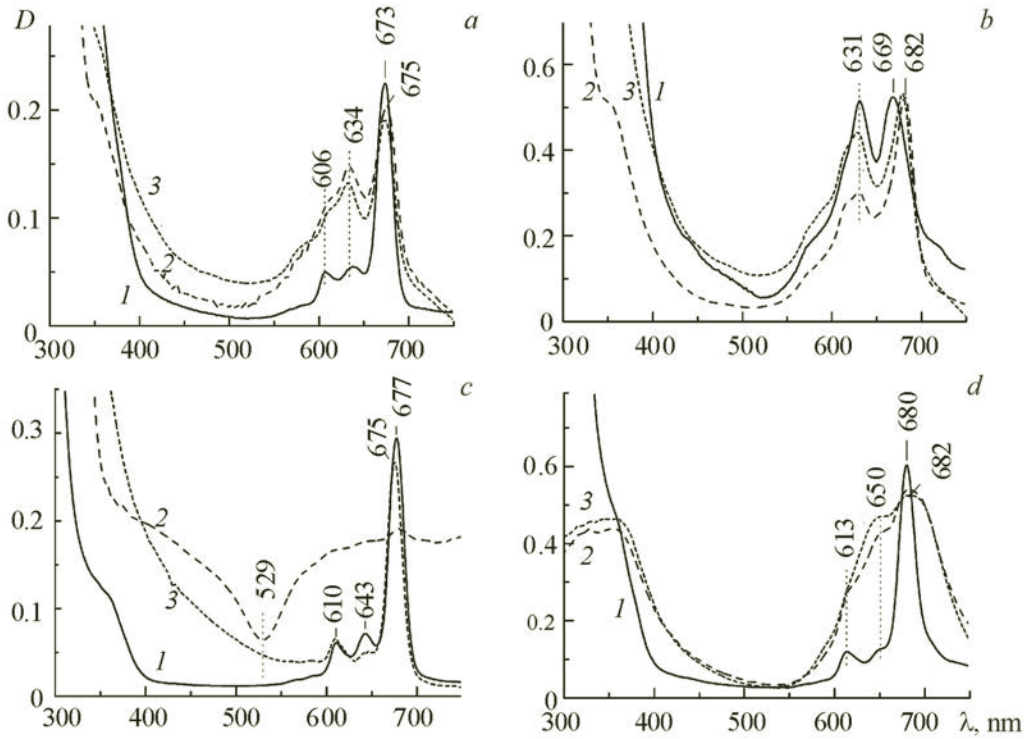

Fig. 3. Electronic absorption spectra of $Si(OH)_2Pc$ (a), $Ge(OH)_2Pc$ (b), AlOHPc (c), and GaOHPc (d) in PVB (1), TEOS (2), and TEOS + VTEOS gel-matrices (3) at 300 K after drying for 60 d.

It was concluded before [12] that $Si(OH)_2Pc$ in acidic solutions could form aggregates with siloxane bonds:

$$n\ Si(OH)_2Pc = HO(SiOPc)_nH + (n-1)H_2O\ ,$$

i.e., aggregates forming polymers through siloxane bonds involving the central Si atom.

The EAS of $Si(OH)_2Pc$ in PVB (Fig. 3a, curve 1) corresponded to the monomeric form with a strong long-wavelength band at 673 nm and was similar in structure to the EAS in solvents (Fig. 1a). A new broad band at 634 nm that corresponded to aggregate absorption (*H*-dimers and more complicated face-to-face structures) according to the literature [27, 30] appeared at shorter wavelengths than the monomeric *Q*(0–0)-band upon incorporating $Si(OH)_2Pc$ into TEOS and TEOS + VTEOS gel-matrices. The new band resulted from the interaction of phthalocyanine rings. Moreover, a weak band at ~720 nm appeared at longer wavelength than the monomer absorption band and could belong to polymeric *J*-aggregates with an edge-to-edge structure [27] that included a large number of phthalocyanine molecules.

Two processes were assumed to be responsible for $Si(OH)_2Pc$ aggregation in the silicate gel matrices. First, the matrix nanopore volume decreased upon drying, thereby increasing the local phthalocyanine concentration within the pores. This was confirmed experimentally because increasing the drying time decreased the nanopore volume and caused the band at 634 nm to grow stronger. Second, $Si(OH)_2Pc$ could interact with pore surfaces containing –OH groups to form a covalent bond with the polymeric framework upon contacting it. This could facilitate aggregation. Furthermore, the intensity of the absorption band at 634 nm depended weakly on the drying time of the TEOS + VTEOS gel-matrix. This may have been due to a lower concentration of surface OH groups in the pores because of the "carpet" of organic vinyl groups.

The stability of the Ge phthalocyanine complex was reduced if Cl^- was replaced by OH^- [31]. It existed in the dissociated state, which deshielded the central atom by removing the counterions and led to aggregate formation. Figure 1b shows that $Ge(OH)_2Pc$ formed *H*-type dimers in DMF. The process was assisted by the solvent coordinating properties (appearance of a strong band at 630 nm). It was concluded before that *Q*-bands for monomeric and dimeric Ge-phthalocyanine had maxima at 668 and 631 nm [30]. This agreed with our data. $Ge(OH)_2Pc$ exhibited analogous EAS in organic PVB polymer (Fig. 3b, curve 1) and DMF solution (Fig. 1b, curve 1). Broadened absorption bands at 668 (669) and 630 (631) nm in DMF (PVB) and their relative intensities were consistent with the existence in these solutions of monomers and dimers of various structures at detectable concentrations. This ratio of $Ge(OH)_2Pc$ spectral forms persisted in the hybrid organo-inorganic

TEOS + VTEOS matrix (Fig. 3b, curve 3). De-aggregation occurred in the inorganic TEOS gel matrix, in contrast with the organic and organo-inorganic media. The increase of relative intensity for the monomer band at 682 nm, its narrowing, and a noticeable bathochromic shift by ~13 nm (Fig. 3b, curve 2) were indicative of this.

Group-IIIA metals (Ga and Al) formed phthalocyanine complexes with monomers that were relatively unstable in the silicate matrices. Thus, the strong *Q*(0–0)-band of monomeric GaOHPc in PVB at 680 nm (Fig. 3d) broadened and shifted to shorter wavelength (~650 nm) in the silicate gel matrices. This indicated that *H*-dimers appeared and increased in concentration (as the gel matrix dried). In parallel, a long-wavelength absorption band (>700 nm) in the region of *J*-aggregates strengthened. Monomeric GaOHPc practically disappeared regardless of the gel matrix (pure TEOS or hybrid TEOS + VTEOS) (Fig. 3d, curves 2 and 3).

The aluminum phthalocyanine complex (AlOHPc) formed a monomer with an absorption band at 677 nm (Fig. 3c, curve 1) in PVB and decomposed in the silicate TEOS matrix. Trace quantities of the monomeric form remained in the inorganic matrix although spectral signatures of aggregates were missing (curve 2). Moreover, the TEOS sample luminesced strongly in the blue-green region. In our opinion, this was the cause of the gap in the absorption spectra at 529 nm (curve 2). Dipyrromethenes are known to fluoresce with high quantum yields in this region. Thus, it could be assumed that the phthalocyanine was destroyed in the TEOS gel to form benzo-derivatives of dipyrromethenes. The EAS of AlOHPc in the hybrid TEOS + VTEOS gel matrix, in contrast with the pure silicate matrix, was identical to the EAS in DMF and EtOH solutions (Fig. 1c). This indicated that only monomeric metal complexes were present in the hybrid organo-inorganic silicate matrix. Thus, a solid-state nanoporous silicate material activated by a monomeric metallophthalocyanine (AlOHPc) that absorbed at the border between the visible and near-IR regions (~675 nm) and had a high fluorescence quantum yield (~0.6 in solvents [32, 33]) was prepared. The border of the near-IR region is 700 nm. However, systems absorbing at shorter wavelengths are usually considered to be in this region [34].

Conclusions. An analysis of solution EAS of mono- and dichlorometallophthalocyanines and their IR spectra showed that the metal complexes were effectively hydrolyzed by atmospheric moisture to form mono- and dihydroxometallophthalocyanines during their synthesis, isolation, and purification, i.e., ligand exchange occurred at the central metal ion. It could be concluded that the two axial ligands in the first coordination sphere of the Group-IVA metal complexes partially protected the complexes from aggregating, as a result of which the monomeric form persisted more than for Group-IIIA metal complexes in the inorganic TEOS matrix. Only AlOHPc remained in the monomeric form in the hybrid TEOS + VTEOS gel matrix. The slightly soluble metal phthalocyanine complexes could be used as dopants in new types of optically isotropic materials based on organic (PVB) and inorganic (TEOS) polymers and hybrid nanocomposite xerogels (TEOS + VTEOS) produced by the sol-gel process. Optically uniform and highly transparent films and matrices with MPc dopant could become a platform for preparing various types of luminescent materials for the visible and near-IR regions.

Acknowledgment. The work was financially supported in part by the Belarusian Republican Foundation for Fundamental Research (Contract No. F16-040).

REFERENCES

1. A. N. Cammidge and R. J. Bushby, in: *Handbook of Liquid Crystals*, D. Demus, J. Goodby, G. W. Gray, H.-W. Spiess, and V. Vill (Eds.), Vol. 2B, Wiley VCH, Weinheim (1998), pp. 693–743.
2. M. Hanack, T. Schneider, M. Barthel, J. S. Shirk, S. R. Flom, and R. G. S. Pong, *Coord. Chem. Rev.*, **219**–**221**, 235–258 (2001).
3. S. R. Flom, in: *The Porphyrin Handbook*, K. M. Kadish, K. M. Smith, and R. Guilard (Eds.), Vol. 19, Academic Press, San Diego (2003), pp. 179–190.
4. G. de la Torre, P. Vazquez, F. Agullo-Lopez, and T. Torres, *Chem. Rev.*, **104**, 3723–3750 (2004).
5. M. Bouvet, *Anal. Bioanal. Chem.*, **384**, 366–373 (2006).
6. A. Sorokin, *Chem. Rev.*, **113**, 8152–8191 (2013).
7. C. G. Claessens, W. J. Blau, M. Cook, M. Hanack, R. J. M. Nolte, T. Torres, and D. Wohrle, *Monatsh. Chem.*, **132**, 3–11 (2001).
8. R. Bonnett, *Chemical Aspects of Photodynamic Therapy*, Gordon and Breach Science Publ., Amsterdam (2000), pp. 199–224.
9. H. Ali and J. E. van Lier, in: *Handbook of Porphyrin Science*, K. M. Kadish, K. M. Smith, and R. Guilard (Eds.), Vol. 4, World Scientific Publ. Co., Singapore (2010), pp. 1–119.
10. S. M. Arabei, T. A. Pavich, and K. N. Solovyov. *J. Porphyrins Phthalocyanines*, **17**, 636–648 (2013).

11. M. K. Lowery, A. J. Starshak, J. N. Esposito, P. C. Krueger, and M. E. Kenney, *Inorg. Chem.*, **4**, 128 (1965).
12. A. S. Akopov, B. D. Berezin, V. N. Klyuev, and A. A. Solov′ev, *Zh. Neorg. Khim.*, **17**, 981–984 (1972).
13. C. W. Dirk, T. Inabe, K. F. Schoch, Jr., and T. J. Marks, *J. Am. Chem. Soc.*, **105**, 1539–1550 (1983).
14. R. D. Joyner and M. E. Kenney, *J. Am. Chem. Soc.*, **82**, 5790–5791 (1960).
15. W. Freyer and Le quoc Minh, *Monatsh. Chem.*, **117**, 475–489 (1986).
16. J. W. Buchler, in: *Porphyrins and Metalloporphyrins*, K. M. Smith (Ed.), Elsevier Scientific Publishing Company, Amsterdam (1975), pp. 157–231.
17. E. A. Luk′yanets (Ed.), *Electronic Spectra of Phthalocyanines and Related Compounds. Catalog. Moscow NPO NIOPIK* [in Russian], NIITEKhIM, Cherkassy (1989).
18. T. Fukuda and N. Kobayashi, in: *Handbook of Porphyrin Science*, K. M. Kadish, K. M. Smith, and R. Guilard (Eds.), Vol. 9, World Scientific Publ. Co., Singapore (2010), pp. 1–644.
19. E. Ciliberto, K. A. Doris, W. J. Pietro, G. M. Reisner, D. E. Ellis, I. Fragala, F. H. Herbstein, M. A. Ratner, and T. J. Marks, *J. Am. Chem. Soc.*, **106**, 7748–7761 (1984).
20. I. Seotsanyana-Mokhosi, N. Kuznetsova, and T. Nyokong, *J. Photochem. Photobiol., A*, **140**, 215–222 (2001).
21. Z. Ou, J. Shen, and K. M. Kadish, *Inorg. Chem.*, **45**, 9569–9579 (2006).
22. T. N. Sokolova, T. N. Lomova, S. V. Zaitseva, S. A. Zdanovich, and V. E. Maizlish, *Russ. J. Inorg. Chem.*, **53**, 220–228 (2008).
23. G. P. Shaposhnikov, V. E. Maizlish, and V. P. Kulinich, *Russ. J. Gen. Chem.*, **75**, 1480–1488 (2005).
24. V. Chauke, A. Ogunsipe, M. Durmuş, and T. Nyokong, *Polyhedron*, **26**, 2663–2671 (2007).
25. M. Durmuş and T. Nyokong, *Polyhedron*, **26**, 3323–3335 (2007).
26. Y. Chen, Y. Araki, M. Fujitsuka, M. Hanack, O. Ito, S. M. O′Flaherty, and W. J. Blau, *Solid State Commun.*, **131**, 773–778 (2004).
27. A. W. Snow, in: *The Porphyrin Handbook*, K. M. Kadish, K. M. Smith, and R. Guilard (Eds.), **17**, Academic Press, San Diego (2003), pp. 129–176.
28. I. Ya. Markova, Yu. A. Popov, and Yu. Kh. Shaulov, *Zh. Fiz. Khim.*, **44**, 2636–2638 (1970).
29. A. S. Akopov, B. D. Berezin, and V. N. Klyuev, *Izv. Vyssh. Uchebn. Zaved., Khim. Khim. Tekhnol.*, **15**, 1190–1192 (1972).
30. A. R. Kane, J. F. Sullivan, D. H. Kenny, and M. E. Kenney, *Inorg. Chem.*, **9**, 1445–1448 (1970).
31. B. D. Berezin and A. S. Akopov, *Zh. Obshch. Khim.*, **44**, 1089–1093 (1974).
32. J. H. Brannon and D. Magde, *J. Am. Chem. Soc.*, **102**, 62–65 (1980).
33. P. C. Martin, M. Gouterman, B. V. Pepich, G. E. Renzoni, and D. C. Schindele, *Inorg. Chem.*, **30**, 3305–3309 (1991).
34. H. Xiang, J. Cheng, X. Ma, X. Zhou, and J. J. Chruma, *Chem. Soc. Rev.*, **42**, 6128–6185 (2013).